Eurasia Journal of Science and Technology
Print ISSN: 2663-1024
Online ISSN: 2663-1016
DOI: https://doi.org/10.61784/ejst3145

POST-TREATMENT STRATEGY: MOLECULAR SIEVE-CONFINED BIFUNCTIONAL METAL-SITE CATALYSTS FOR HYDROGEN PRODUCTION FROM FORMIC ACID DECOMPOSITION

LeBin Mi, Ning Wang, Tao Cai*
College of Chemistry and Chemical Engineering, Qingdao University, Qingdao 266071, Shandong, China.
**Corresponding Author: Tao Cai*

Abstract: Formic acid, as an important liquid organic hydrogen carrier, is considered a highly promising chemical medium for hydrogen storage due to its high hydrogen storage density, safety, non-toxicity, and ease of storage and transportation. It can also catalytically decompose to release hydrogen under mild conditions. However, traditional supported noble metal catalysts face issues such as metal nanoparticle migration, agglomeration, and leaching during the reaction process, leading to reduced catalyst activity and instability. To address these challenges, this thesis utilizes the microporous confinement effect of molecular sieves to design and prepare a series of Pd-based catalysts confined within molecular sieves. The catalytic performance, kinetic behavior, and cycle stability of these catalysts were systematically investigated. Various characterization techniques were used to elucidate the relationship between catalyst structure and performance. Using a commercial Beta molecular sieve as the carrier, acidic sites were removed through aluminophosphoric acid treatment. Then, highly dispersed Pd nanoclusters confined within the molecular sieve pores were successfully synthesized using a combination of ligand protection and hydrogen reduction after calcination. A second metal, Ce, was subsequently introduced to create the PdCe-Beta-DeAL-C-H bimetallic catalyst. Characterization results showed that aluminophosphoric acid treatment and the addition of Ce effectively improved the dispersion and stability of the Pd particles. The Pd nanoparticles had a small size of 2–5 nm and were uniformly distributed on the surface of the carrier and near its pores. Ce was in close contact with Pd, and the interfacial interactions altered the surface electronic structure of Pd, thereby promoting the formation and stabilization of metallic Pd^0. Catalytic tests demonstrated that the optimal $Pd_{1.0}Ce_{0.2}$-Beta-DeAL-C-H catalyst achieved a conversion rate of 3199 $molH_2 \cdot molPd^{-1} \cdot h^{-1}$ at 60 °C during formic acid decomposition. This value was approximately 127% higher than that of the single-metal catalyst. Additionally, the catalyst exhibited excellent cycle stability: after five cycles, its conversion rate remained above 1800 $molH_2 \cdot molPd^{-1} \cdot h^{-1}$. Kinetic studies revealed that the apparent activation energy for formic acid decomposition over this catalyst was 55.93 $kJ \cdot mol^{-1}$, significantly lower than that of the catalyst without Ce (84.5 $kJ \cdot mol^{-1}$). Moreover, the catalyst performed well in the reaction of CO_2 hydrogenation to formic acid, with a reaction rate of 62 $molformate \cdot molPd^{-1} \cdot h^{-1}$. This study demonstrates that the incorporation of Ce through post-treatment effectively enhances the performance of Pd-based catalysts for formic acid decomposition. It provides valuable insights for the design of efficient bimetallic catalysts.
Keywords: Pd nanocatalyst; Bimetallic synergy; Molecular sieve confinement; Formic acid decomposition

1 INTRODUCTION

Hydrogen, as an efficient and clean secondary energy carrier, is one of the ideal solutions to address the energy crisis and environmental issues[1-2]. However, the safe and efficient storage and controlled release of hydrogen remain key technological bottlenecks for its large-scale application[3]. Liquid organic hydrogen carriers have attracted widespread attention due to their high hydrogen storage density, excellent transportation safety, and potential for controlled hydrogen release under mild conditions. Among them, formic acid is regarded as one of the most promising liquid hydrogen storage media, owing to its high mass-based hydrogen storage density (4.4 wt%)[4], non-toxicity, stability as a liquid at room temperature and atmospheric pressure, and ease of regeneration. Through catalytic decomposition, formic acid can selectively release H_2 and CO_2 under mild conditions, providing an efficient solution for on-site, on-demand hydrogen supply [5-6].

The core of formic acid decomposition for hydrogen production lies in the design of high-performance catalysts. Noble metal catalysts, especially nanomaterials based on Pd, Pt, and Au, have demonstrated excellent catalytic activity in this reaction. However, noble metal nanoparticles prepared by traditional methods are prone to migration, agglomeration [7], and even leaching during the reaction, leading to a reduction in active sites and a sharp decline in catalytic stability. Additionally, the high cost associated with high metal loading limits their practical application. Therefore, developing catalytic systems capable of stabilizing and highly dispersing metal active centers while achieving high activity, high selectivity, and long-term stability has become a key research focus in this field [8-9].

In recent years, porous material-confined metal catalysts have shown great potential in the catalytic decomposition of liquid hydrogen storage molecules due to their unique spatial confinement effects and tunable support properties [10-11]. Among them, zeolites, with their ordered microporous channels, high specific surface area, tunable acidity/alkalinity, and excellent hydrothermal stability, are considered ideal supports for achieving atomic-level dispersion and strong anchoring

of metal species. The pore confinement effect of zeolites can effectively inhibit the agglomeration of metal nanoparticles during preparation and reaction, while the strong interaction between the metal and the support framework (such as silanol groups and aluminum sites) can further modulate the electronic structure of active centers and optimize the reaction pathway [12]. Studies have shown that encapsulating ultrafine noble metal nanoclusters within zeolite pores not only significantly enhances metal dispersion and stability but also substantially improves intrinsic catalytic activity through metal-support synergistic effects.

This work aims to leverage advanced zeolite confinement synthesis strategies to design and prepare a series of efficient and stable zeolite-encapsulated ultrafine metal catalysts for formic acid decomposition for hydrogen production. By tuning the pore structure and surface properties (e.g., hydrophobicity, acidic sites) of the zeolite supports and incorporating synergistic promoters (such as Ce), we systematically investigate the structure-performance relationships between catalyst structure (metal dispersion, particle size, electronic state) and catalytic performance (activity, selectivity, stability). The goal is to develop a new generation of formic acid decomposition catalysts with low noble metal loading, high activity, high selectivity (suppression of CO byproducts), and excellent stability, thereby providing technical support for the convenient and safe utilization of hydrogen energy.

2 MATERIALS AND METHODS

2.1 Materials

The experimental reagents included: formic acid (85% purity), nitric acid (99% purity), sodium borohydride, anhydrous ethylenediamine (99.7% purity), and cerium nitrate, all purchased from Sinopharm Chemical Reagents Co., Ltd. The commercially available Beta-25 molecular sieve was acquired from Luoyang Jianlong Micro-Nano New Materials Co., Ltd. Palladium chloride, manganese chloride hexahydrate, and cobalt nitrate hexahydrate were purchased from McLean. Sodium formate was bought from Aladdin. Deionized water was provided by Qingdao Xinda Sheng Chemical Reagents Co., Ltd.

2.2 Synthetic Methods

Preparation of Pd(en)2Cl2 solution: Using a pipette, add 1 mL of ethylenediamine solution to 10 mL of aqueous solution. Then add 0.3195 g of PdCl2 powder. Stir at 1000 rpm for 30 minutes until the powder dissolves. The resulting solution is a 0.18 M Pd(en)2Cl2 solution.

Alumina removal from Beta molecular sieve: First, take an appropriate amount of commercial Beta molecular sieve powder and place it in a crucible. Calcine it in a muffle furnace at 550 °C in air for 3 hours. After cooling to room temperature, mix the powder with 25 mL of 12 M nitric acid in a round-bottom flask. Place the mixture in an oil bath at 80 °C and stir at 800 rpm under reflux for 8 hours. Transfer the liquid to 50 mL centrifuge tubes. Wash the mixture with water using a centrifuge until the wash liquid is neutral (tested with pH paper). Then freeze-dry the solid powder in a freeze dryer for 6 hours or longer until completely dry. Place the dried powder back in a muffle furnace and heat it to 550 °C over 6 hours. Hold at this temperature for 3 hours before cooling. The resulting material is Beta-DeAL, the alumina-removed Beta molecular sieve.

Synthesis of Pd1%-Beta-DeAL-C-H catalyst: In a 50 mL centrifuge tube, add 0.5 g of Beta-DeAL carrier and 5 mL of distilled water. Ultrasonicate for 30 minutes to ensure the carrier is evenly dispersed in the water. Add a 15 mm rotor and stir at 800 rpm for 5 minutes. Then add 0.21 mL of 0.18 M Pd(en)2Cl2 solution and continue stirring at 800 rpm for 2 hours. Centrifuge at 8000 rpm for 8 minutes. Reduce the supernatant with 1 M sodium borohydride solution. If a black precipitate forms, it indicates that not all of the Pd metal has entered the pores of the Beta molecular sieve. If no precipitate forms, it means all the Pd metal has been adsorbed onto the Beta molecular sieve. Freeze-dry the white solid obtained after centrifugation for 6 hours or longer until completely dry. This gives Pd1%-Beta-DeAL solid powder. Place this powder in a muffle furnace and heat it to 500 °C for 3 hours. After cooling, reduce it with H2 at 30 mL·min-1 at 400 °C for 2 hours to obtain Pd-Beta-DeAL-C-H catalyst.

Synthesis of PdCe-Beta-DeAL-C-H catalyst: Place 1 g of the freshly synthesized Pd-Beta-DeAL-C solid powder in an oven at 80 °C for 30 minutes. Then, using the impregnation method, add cerium nitrate solution to the powder while stirring at 800 rpm for 2 hours. Freeze-dry the mixture until completely dry. Finally, reduce it with H2 at 30 mL·min-1 at 400 °C for 2 hours to obtain PdCe-Beta-DeAL-C-H catalyst. Repeat the procedure to prepare samples with Pd:Ce ratios of 1:0.1, 1:0.2, 1:0.5, and 1:1. These samples are named Pd1Cex-Beta-DeAL-C-H (where X = 0.1, 0.2, 0.5, 1).

2.3 Characterizations

The obtained catalysts were scanned using an X-ray diffractometer (Ultima IV) over a range of diffraction angles (2θ) from 5° to 80° at a scanning rate of 5°/min. This allowed for the characterization of the material's crystal structure and phase composition. Transmission electron microscopy (TEM, Thermo Fisher TF20, equipped with an EDAX spectrometer) was used to observe the microscopic morphology and structural details of the samples, as well as to analyze their elemental distribution. In-situ infrared spectroscopy was performed using the FOLI10-R instrument. The chemical composition of the synthesized catalysts and their products was determined, and the resulting electron energy spectra were analyzed. A fully automatic program-controlled temperature chemisorption apparatus was used to conduct CO pulse adsorption tests on the synthesized catalysts, thereby determining the dispersion of Pd elements within the catalyst.

3 RESULTS AND DISCUSSION

3.1 Structure of the Catalyst

First, we used commercial Beta molecular sieve as a carrier. Through preliminary alumina-removal treatment, a large number of acidic sites on the surface of the carrier were removed. Then, monometallic Pd was coupled to the carrier using ligand protection methods. After calcination, hydrogen reduction was used to incorporate the Pd into the H-type molecular sieve structure of the Beta molecular sieve. Additionally, the second metal Ce was introduced to improve the electronic transition state of the Pd atoms. This combination of effects from both metals and the constraints imposed by the molecular sieve significantly enhanced the hydrogen production efficiency during formic acid decomposition (Figure 1).

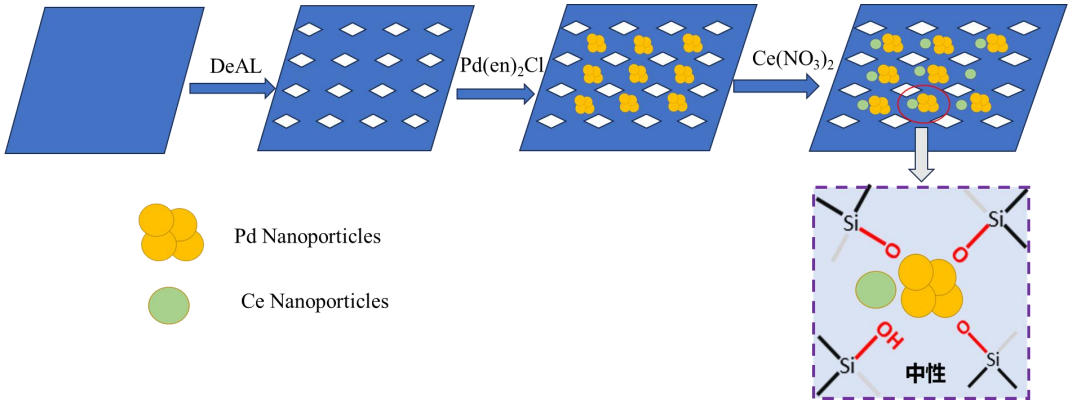

Figure 1 Schematic Diagram of H-Type Zeolite Nanosheets Loaded with Pd Nanoparticles

For comparison, catalysts were also prepared without the addition of the second metal catalyst Pd-Beta-DeAL-C-H, those that were not calcined at 500°C in air (Pd-Beta-DeAL-H), those where the carrier had not undergone alumina removal treatment (Pd-Beta-C-H), and those where neither alumina removal nor calcination was performed on the carrier (Pd-Beta-H). Powder X-ray diffraction patterns confirmed that the BEA molecular sieve structure remained intact, indicating that the alumina removal and subsequent treatment processes did not damage the main framework of the Beta molecular sieve. In contrast, there were significant differences in the diffraction patterns of the Pd species across the samples: In Pd-Beta-H, clear and sharp Pd peaks appeared at around $2\theta=40.1°$ and 46.6°, suggesting that without alumina removal, Pd tended to form larger particles and aggregate. After alumina removal, the Pd peaks in Pd-Beta-DeAL-H became weaker and broader, indicating that the size of the Pd particles decreased and their dispersion improved. In Pd-Beta-DeAL-C-H after calcination and reduction, as well as in PdCe-Beta-DeAL-C-H with Ce added, the Pd peaks completely disappeared, indicating that the Pd species existed in the form of ultra-fine nanoparticles or was highly dispersed on the surface and within the pores of the carrier. High-resolution STEM images of the Pd-Ce bimetallic catalyst also show that its metal components remain well-dispersed on the Beta molecular sieve substrate. Images at various scales demonstrate that, whether at 100 nm, 50 nm, or 20 nm, the bright white metal particles exhibit a fine and uniform distribution, with no signs of large particle aggregation. Even under high magnification, the metal particles maintain good size uniformity, indicating that the addition of Ce did not disrupt the highly dispersed structure of the Pd species. Compared to the particle growth commonly observed in Pd/Beta catalysts prepared by traditional impregnation methods, the Pd-Ce/Beta-DeAL-C-H sample exhibits superior metal dispersion, suggesting that the post-treatment strategy, combined with the confinement effect of the molecular sieve, effectively stabilizes the bimetallic components. Further analysis using energy-dispersive X-ray spectroscopy (EDX) mapping revealed that Pd is uniformly distributed across the Beta-DeAL substrate, with no evidence of localized enrichment. This indicates that Pd species are highly dispersed both on the surface and within the pores of the molecular sieve. This finding corroborates the results of the STEM analysis, confirming that the alumina-removed and post-treated Beta molecular sieve provides an ideal environment for Pd species, thereby preventing particle aggregation. Meanwhile, Ce is also evenly distributed on the substrate and shows a high degree of spatial co-localization with Pd, indicating that the Ce species introduced during post-treatment form a closely bonded bimetallic interface with Pd. This spatial proximity facilitates potential electronic interactions and synergistic effects between Pd and Ce, thereby enhancing the interaction between the active components and the substrate and improving the stability of the metal species during the reaction (Figure 2).

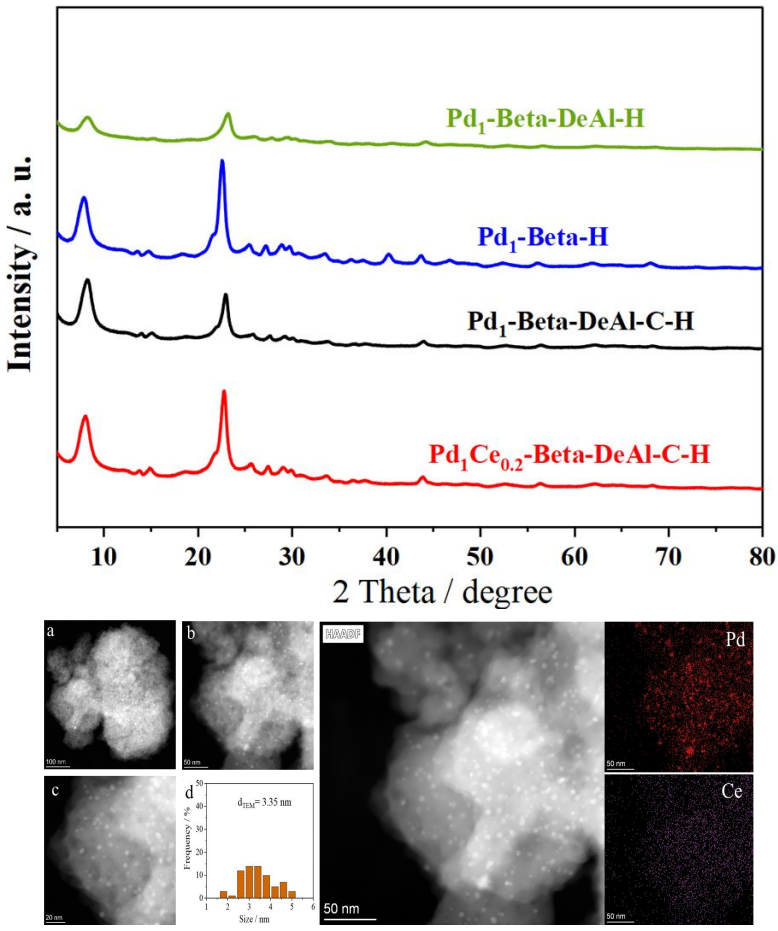

Figure 2 XRD Patterns, STEM Images and Particle Size Distributions of Palladium Nanoparticles Supported on Beta Zeolite, along with (EDX) Mapping

As calculated from the CO pulse adsorption results in Figure 3(a), the dispersion degree of Pd in the PdCe-Beta-DeAL-C-H catalyst was 11.2%, indicating that Pd species are highly dispersed on the catalyst surface. In conjunction with the fact that no distinct Pd-related diffraction peaks were observed in the XRD results, and the uniform distribution of Pd and Ce components as confirmed by STEM and EDX mapping, it can be inferred that Pd exists primarily in the form of ultra-fine nanoparticles or is highly dispersed on the Beta-DeAL substrate. This indicates that the beta molecular sieve, after alumina removal, calcination, and reduction treatment, provides an effective environment for Pd species to be confined and stabilized. The addition of Ce further enhances the stability and dispersion of Pd, thereby preventing its migration and agglomeration during thermal treatment and reaction processes. Overall, the CO pulse adsorption results confirm that the PdCe-Beta-DeAL-C-H catalyst possesses numerous accessible surface active sites, which provides a structural basis for the excellent catalytic activity and stability of the Pd-Ce bimetallic system in formic acid decomposition reactions. Figure 3(b) shows that, compared to the single Pd catalyst, the PdCe-Beta-DeAL-C-H catalyst with Ce added exhibits stronger and sharper infrared absorption peaks in the 2100–2000 cm-1 range. This indicates an increase in the number of Pd active sites capable of adsorbing CO, along with higher Pd dispersion and a more uniform surface structure. These absorption peaks correspond to CO molecules linearly adsorbed on the Pd surface. The enhanced peak intensity suggests that the addition of Ce effectively alters the surface electronic structure of Pd, improving the accessibility and exposure of the active sites..

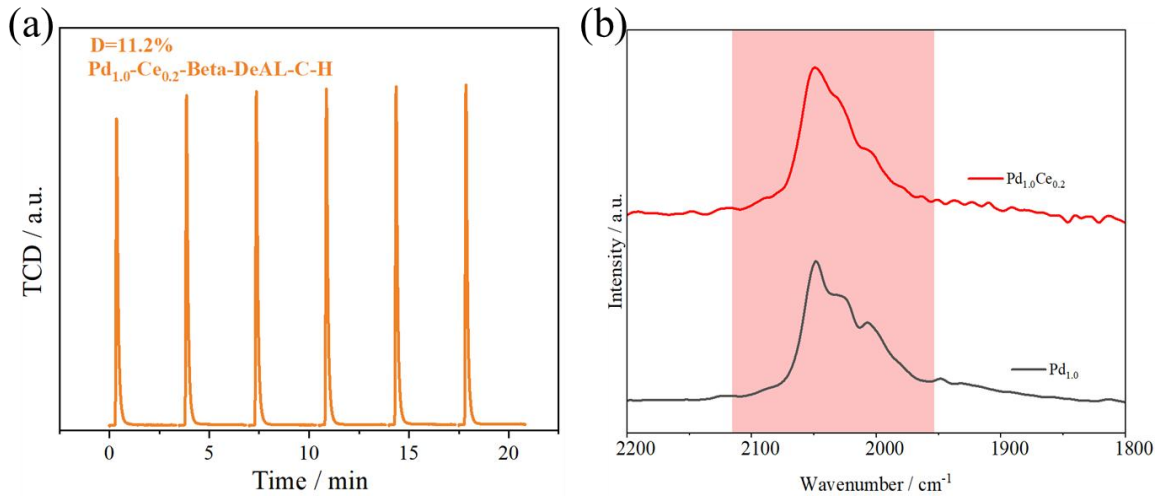

Figure 3 (a) CO Pulse Adsorption Curves of the PdCe-Beta-DeAL-C-H Catalyst; (b) CO-FTIR Spectra of PdCe-Beta-DeAL-C-H and Pd-Beta-DeAL-C-H

As shown in Figure 4.(a), the Pd 3d XPS spectra of samples (c) PdCe-Beta-DeAL-C-H and (b) Pd-Beta-DeAL-C-H are presented. XPS analysis revealed significant differences in the chemical state of palladium (Pd) between these two samples. In the PdCe-Beta-DeAL-C-H sample, strong Pd0 peaks were observed at around 335.1 eV and 340.3 eV, while weaker Pd2+ peaks appeared at approximately 337.2 eV and 342.4 eV. This indicates that the Pd species in this sample predominantly exist in a metallic state, with only a small amount present in oxidized form. In contrast, in the Pd-Beta-DeAL-C-H sample, the intensity of the Pd2+ peaks was significantly higher, whereas the Pd0 peaks were relatively weak. This suggests that the Pd species on its surface were mainly in oxidized form, with a lower content of metallic Pd. These results indicate that the addition of CeOx effectively promoted the reduction of Pd species and increased the stability of the metallic Pd0 state. This is likely due to CeOx's rich oxygen vacancies and reversible Ce3+/Ce4+ redox properties, which allow it to regulate the local electronic environment around Pd, thereby enhancing its reducibility and optimizing the structure of the active site. Therefore, the higher proportion of metallic Pd0 in the PdCe-Beta-DeAL-C-H sample is one of the key reasons for its higher catalytic activity in formate decomposition reactions.

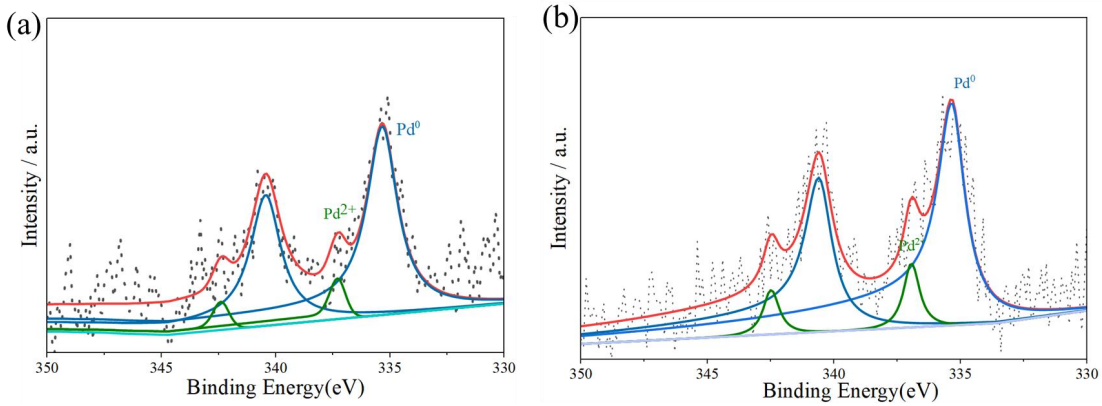

Figure 4 XPS Spectra of (a) PdCe-Beta-DeAL-C-H and (b) Pd-Beta-DeAL-C-H

3.2 Catalytic Performances

To systematically evaluate the catalytic performance of the prepared catalysts in the hydrogen production reaction from formic acid decomposition, this section conducted activity tests on different samples under identical reaction conditions. The reaction conditions were as follows: 3 mmol of formic acid and sodium formate were used, with a molar ratio of precious metal to formic acid of 0.002. The reaction temperature was 60 ℃ at atmospheric pressure.

For single-metal catalysts, the catalytic activities of catalysts with Pd loaded under various treatment conditions and loading methods were tested at room temperature, as shown in Figure 5.a. The Pd-Beta-DeAL-C-H catalyst exhibited extremely high catalytic activity for formic acid decomposition. It could produce 147 mL of gas within 9 minutes, with a turnover frequency (TOF) of 1403 molH2·molPd-1·h-1. This value is 5.3 times higher than that of Pd-Beta-DeAL-H (263 molH2·molPd-1·h-1), 1.3 times higher than Pd-Beta-C-H (1052 molH2·molPd-1·h-1), and 9.95 times higher than Pd-Beta-H (141 molH2·molPd-1·h-1). This confirms that the aluminophosphate removal from the carrier makes the catalytic environment more neutral, thereby facilitating formic acid decomposition and enhancing catalytic activity. Additionally, post-sintering reduction treatment improved both the structure and performance of the catalyst.

Further studies were conducted to investigate the synergistic catalytic effect of bimetallic clusters on hydrogen production from formic acid decomposition. The effects of different metal dopants on catalyst performance were examined. In Figure 5.b, the PdCe-Beta-DeAL-C-H catalyst showed the fastest gas generation rate, producing 147 mL of gas in just 3 minutes, far exceeding that of other catalysts. This indicates its superior catalytic kinetics. The TOF of PdCe was as high as 3199 molH2·molPd-1·h-1, significantly higher than that of PdNi (2638 molH2·molPd-1·h-1), PdMn (690 molH2·molPd-1·h-1), and PdCo (1319 molH2·molPd-1·h-1). This confirms that the addition of Ce significantly enhances catalyst activity.
To further understand the synergistic catalytic effect of Pd-Ce bimetallic clusters and improve hydrogen production efficiency from formic acid decomposition, systematic tests were performed using Pd1.0Cex-Beta-DeAL-C-H catalysts with varying Ce contents to determine the optimal Pd/Ce molar ratio. As shown in Figure 5.c, the total volume of CO2 and H2 generated over time varied significantly among catalysts with different Pd-Ce molar ratios, indicating that Ce content has a significant impact on catalyst performance. When the Ce content was 0.2, the Pd1.0Ce0.2-Beta-DeAL-C-H catalyst exhibited the best performance. It produced 147 mL of gas in about 3 minutes, with a TOF of 3199 molH2·molPd-1·h-1. In contrast, when the Ce content was lower or higher than this ratio, both the gas generation rate and TOF decreased significantly. This shows that there is an optimal range for Ce content. Appropriate Ce doping can effectively regulate the electronic structure and local coordination environment of Pd active sites, enhance the interaction between the metal and the carrier, and promote the stable dispersion of active components. This, in turn, significantly improves the efficiency of formic acid decomposition catalysis. Excessive Ce doping, however, may cover some Pd active sites or disrupt the existing electronic balance and interface structure, leading to a decline in catalytic performance. This clearly demonstrates that appropriate Ce doping plays a crucial role in enhancing the hydrogen production performance of Pd-based catalysts for formic acid decomposition..

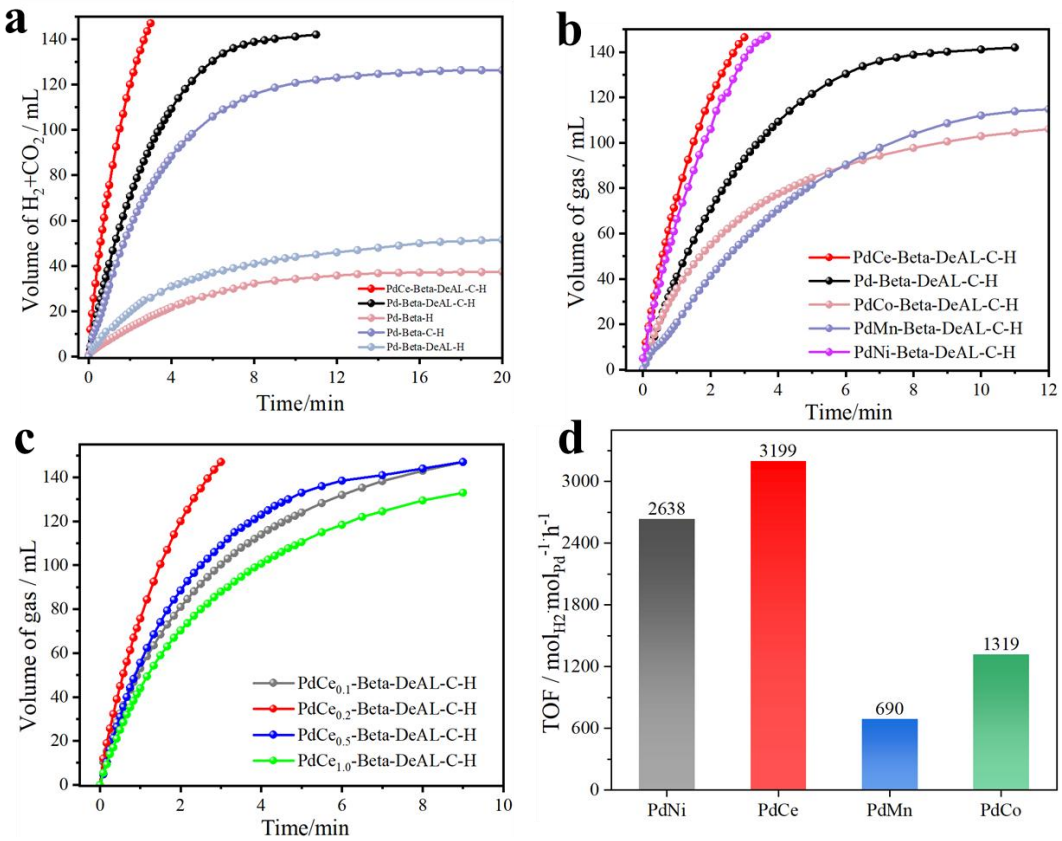

Figure 5 a) Hydrogen Generation Performance of Formic Acid Decomposition over Pd-Beta-DeAL-C-H, Pd-Beta-H, Pd-Beta-C-H, and Pd-Beta-DeAL-H Catalysts; b) Volume of Gas Produced over Time from the Decomposition and Dehydrogenation of formic Acid at 60°C Using Different Pd-Beta-DeAL-C-H bimetallic Catalysts ; c) Volume of Gas Generated over Time from the Decomposition and Dehydrogenation of Formic Acid at Room Temperature Using Pd1.0Cex-Beta-DeAL-C-H Catalysts with Varying Ce Contents; d) TOF Corresponding to Different Bimetallic Catalysts

To further investigate the kinetic properties of catalysts in the hydrogen production reaction from formic acid decomposition, the catalytic performance of the Pd1.0Ce0.2-Beta-DeAL-C-H catalyst was examined at various reaction temperatures. As shown in Figure 6.a, as the reaction temperature decreased from 333 K to 313 K, the catalyst's activity for formic acid decomposition significantly declined. This was manifested by a gradual decrease in gas production per unit time, a significant reduction in the hydrogen generation rate during the initial stages of the reaction, and an increased time required to reach the reaction endpoint. Correspondingly, the TOF value of the catalyst also decreased with decreasing temperature, from 3199 molH2·molPd-1·h-1 at 333 K to 910 molH2·molPd-1·h-1 at 313 K. These results

indicate that increasing the reaction temperature accelerates the rate of formic acid decomposition. The Pd1.0Ce0.2-Beta-DeAL-C-H catalyst maintains high activity even at higher temperatures, demonstrating its excellent thermal stability. This stability is attributed to the confinement and stabilization effect of the Beta molecular sieve support on the Pd-Ce bimetallic species, thereby preventing the migration, aggregation, and deactivation of the active metal components during the reaction. Kinetic modeling of the formic acid decomposition reaction using the Arrhenius equation is shown in Figure 6.b. Linear regression analysis yielded an apparent activation energy of 55.93 kJ·mol-1 for the PdCe-Beta-DeAL-C-H catalyst, which is significantly lower than 84.5 kJ·mol-1 for the Pd-Beta-DeAL-C-H catalyst, representing a reduction of approximately 33.8%. This indicates that the Pd-Ce bimetallic interaction effectively reduces the energy barrier for formic acid decomposition, thereby enhancing the hydrogen production process. Additionally, XPS analysis revealed that the addition of CeOx altered the electronic structure of the Pd species, increased the proportion of metallic Pd, and optimized the local electronic environment around the active sites. This facilitated the adsorption and activation of formic acid molecules and the subsequent conversion of formate intermediates. In summary, the Pd-Ce bimetallic interaction not only enhances the catalyst's intrinsic activity but also provides a kinetic basis for efficient hydrogen production from formic acid decomposition under mild conditions.

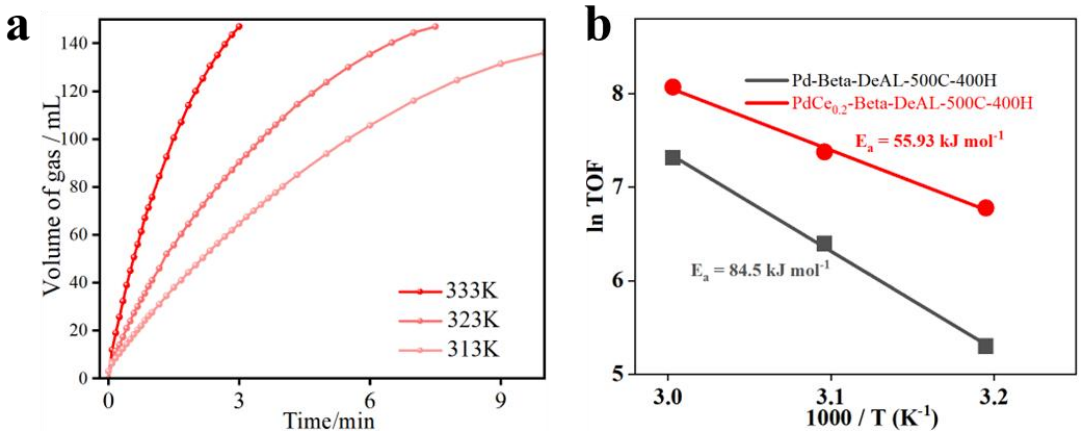

Figure 6 (a) Volume of Gas Produced from Formic Acid Decomposition at Different Temperatures over Time Using the $Pd_{1.0}Ce_{0.2}$-Beta-DeAL-C-H Catalyst; (b) Arrhenius Plots for Hydrogen Evolution from Formic Acid Decomposition over PdCe-Beta-DeAL-C-H and Pd-Beta-DeAL-C-H Catalysts at Different Temperatures

To verify the cyclic stability of the catalyst in the hydrogen production reaction from formic acid decomposition, five repeated catalytic tests were conducted at 60 °C using the Pd1.0Ce0.2-Beta-DeAL-C-H catalyst. Each cycle involved the use of a freshly prepared 6 M formic acid/sodium formate solution. As shown in Figure 7, during the five consecutive formic acid decomposition reactions, the gas production curves of the Pd1.0Ce0.2-Beta-DeAL-C-H catalyst remained relatively consistent. The change in gas volume over time was minimal, and gas release was completed within approximately 4 minutes in all cases. This indicates that the catalyst retained its excellent catalytic activity and reusability after multiple cycles. Although there was a slight decrease in catalytic activity with increasing cycle numbers, the overall change was minimal. This may be due to the accumulation of $HCOO^-$ and Na^+ ions on the catalyst surface, thereby partially blocking some active sites. Overall, these results demonstrate that the pore-limiting effect of the Beta molecular sieve effectively prevents the migration and agglomeration of metal active components during the reaction, maintaining their high dispersion and uniform distribution. This ensures the continuous and stable operation of the catalyst. Morphological analysis of the catalyst after multiple cycles is shown in Figure 8. After five formic acid decomposition reactions, the Pd1.0Ce0.2-Beta-DeAL-C-H catalyst still maintained good structural stability. The Pd nanoparticles remained uniformly dispersed on the carrier surface with sizes ranging from 2 to 5 nm. Slight agglomeration or sintering was observed, which led to a decrease in formic acid decomposition activity. However, the catalyst still exhibited a high reaction rate. This suggests that the addition of Ce as a promoter, along with the pore-limiting effect of the Beta molecular sieve, effectively stabilized the Pd active species and prevented their deactivation during the reaction. Thus, these morphological findings provide direct evidence that the catalyst retains high activity even after multiple cycles.

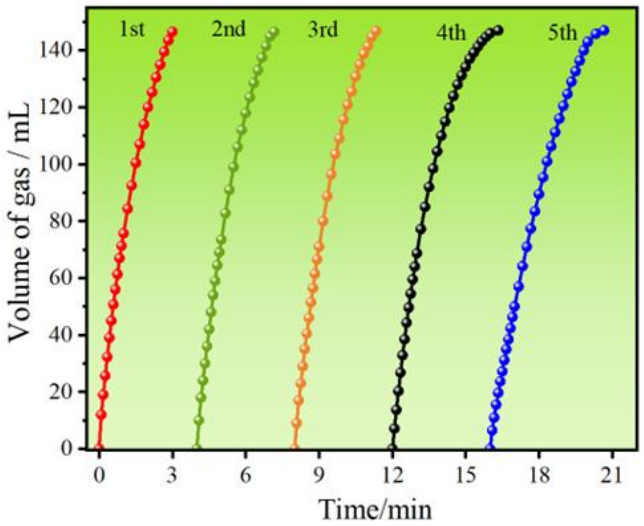

Figure 7 Hydrogen Production Performance Chart for Formic Acid Decomposition Cycle Tests on Pd1.0Ce0.2-Beta-DeAL-C-H Catalyst at 60℃

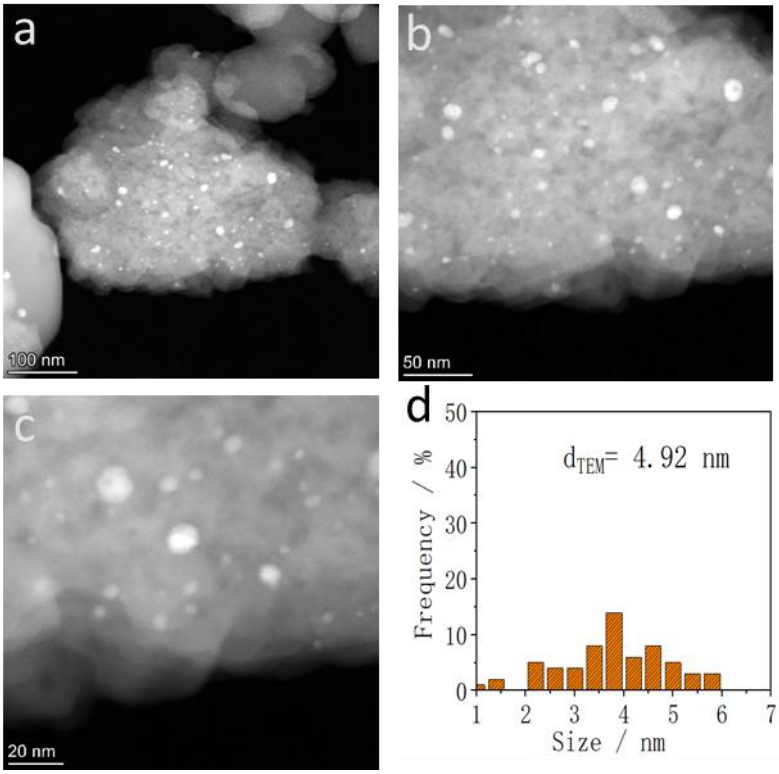

Figure 8 High-Resolution STEM Images and Particle Size Distribution of the Pd1.0Ce0.2-Beta-DeAL-C-H Catalyst after the Fifth Formic Acid Decomposition Reaction

4 CONCLUSION

In this study, Beta molecular sieve was used as the carrier. After alumina removal and subsequent reduction treatment following calcination, a pore structure was created that facilitated high-dispersion loading and stable retention of metals. Ce was introduced using a post-modification impregnation method, resulting in the successful preparation of the PdCe-Beta-DeAL-C-H bimetallic catalyst. Characterization studies using XRD, STEM, EDX mapping, CO pulse adsorption, and XPS revealed that both the alumina removal process and the addition of Ce improved the dispersion of Pd particles and enhanced their stability. The Pd nanoparticles were uniformly distributed on the surface of the carrier and within its pores, maintaining small sizes and high dispersion. Additionally, Ce and Pd were in close spatial proximity, and their interfacial interactions altered the surface electronic structure of Pd, thereby promoting the formation and stabilization of metallic Pd. This provided a structural foundation for creating highly efficient bimetallic catalysts.

Catalytic performance tests showed that the amount of Ce added had a significant effect on hydrogen production from formic acid decomposition. The Pd1.0Ce0.2-Beta-DeAL-C-H catalyst performed best, achieving a TOF of 3199 molH2·molPd-1·h-1 at 60 °C, which is approximately 127% higher than that of the single-metal Pd1.0-Beta-DeAL-C-H

catalyst. This catalyst also exhibited excellent catalytic efficiency in converting CO2 to formic acid, with a rate of 62 molformate·molPd-1·h-1. Kinetic studies indicated that the apparent activation energy for formic acid decomposition over this catalyst was 55.93 kJ·mol-1, significantly lower than 84.5 kJ·mol-1 for the Pd-Beta-DeAL-C-H catalyst. This suggests that the synergistic effect between Pd and Ce effectively reduced the reaction barrier, facilitating the adsorption and conversion of formic acid molecules. Cycle stability tests confirmed that the catalyst retained high activity after five consecutive reactions. The gas production curves remained consistent, and the Pd particles continued to be uniformly dispersed at small sizes of 2–5 nm, with no signs of agglomeration or sintering. In conclusion, this study demonstrates that the incorporation of Ce through post-treatment effectively enhances the activity and stability of Pd-based catalysts supported on molecular sieves, providing a valuable basis for designing highly efficient catalysts for hydrogen production from formic acid decomposition..

COMPETING INTERESTS

The authors have no relevant financial or non-financial interests to disclose.

ACKNOWLEDGMENTS

The authors thank the support by Qingdao Xinding Wanxing New Materials Co., Ltd.

REFERENCES

[1] Nejat P, Jomehzadeh F, Taheri M M, et al. A global review of energy consumption, CO2 emissions and policy in the residential sector (with an overview of the top ten CO2 emitting countries). Renewable and Sustainable Energy Reviews, 2015: 43843-862.
[2] Zhou J, Zhang W, Cai W, et al. High stability for the integrated CO2 capture and methanation reaction over the MgO-modified Ni-CaO bifunctional catalyst. Separation and Purification Technology, 2025: 366132845.
[3] Li K, Dong X, Wang H, et al. Study on the influence factors of gravimetric hydrogen storage density of type III cryo-compressed hydrogen storage vessel. International Journal of Hydrogen Energy, 2024: 96680-691.
[4] Liu P, Wang Y, Zhou Z, et al. Effect of carbon structure on hydrogen release derived from different biomass pyrolysis. Fuel, 2020: 271117638.
[5] Sun Q, Wang N, Xu Q, et al. Nanopore-supported metal nanocatalysts for efficient hydrogen generation from liquid-phase chemical hydrogen storage materials. Advanced Materials, 2020, 32(44): 2001818.
[6] Ma H Z, Canty A J, O'hair R a J. Liberation of carbon monoxide from formic acid mediated by molybdenum oxyanions. Dalton Transactions, 2023, 52(43): 15734-15746.
[7] Zhu Q L, Tsumori N, Xu Q. Sodium hydroxide-assisted growth of uniform Pd nanoparticles on nanoporous carbon MSC-30 for efficient and complete dehydrogenation of formic acid under ambient conditions. Chemical Science, 2014, 5(1): 195-199.
[8] Liu C, Lei T, Wang Y, et al. Ceratostigma willmottianum mineralizes atmospheric carbon dioxide into calcium carbonate in a high-calcium environment. Plant Physiology, 2025, 197(4): kiaf134.
[9] Wang N, Sun Q, Bai R, et al. American Chemical Society, 2016, 138: 7484-7487.
[10] Wang X, Zhang Y, Liang H, et al. Catalytic hydrogenolysis of formic acid to hydrogen over heterogeneous catalysts: A review on modification strategies, catalyst deactivation and reaction mechanism. Applied Catalysis A: General, 2024: 687119972.
[11] Pan Y, Pan C L, Zhang Y, et al. Selective hydrogen generation from formic acid with well-defined complexes of ruthenium and phosphorus–nitrogen PN3-pincer ligand. Chemistry – An Asian Journal, 2016, 11(9): 1357-1360.
[12] Wang A, He P, Wu J, et al. Reviews on homogeneous and heterogeneous catalysts for dehydrogenation and recycling of formic acid: progress and perspectives. Energy & Fuels, 2023, 37(22): 17075-17093.